ELSEVIER

Int. J. Therm. Sci. 41 (2002) 401–411

International Journal of Thermal Sciences

www.elsevier.com/locate/ijts

Modeling of the radiative contribution to heat transfer in porous media composed of spheres or cylinders

Pablo Rubiolo [a,b,*], Jean-Marie Gatt [c]

[a] *DRN/DER/SERI, CEA-Cadarache, 13108, St Paul Lez Durance, France*
[b] *Westinghouse Electric Company, Building 401, Room 2 A7, 1340 Beulah Road, Pittsburgh, PA 15235, USA*
[c] *DEC/SESC/LLCC- bât 315, CEA-Cadarache, 13108, St Paul Lez Durance, France*

Received 2 November 1999; accepted 12 September 2001

Abstract

A theoretical model for evaluating the radiative conductivity tensor of a porous media is developed in this paper. The porous media is composed of a transparent fluid and opaque particles with characteristic lengths longer than the radiation wavelength. The main features of the proposed approach are (i) take into account the interaction between conduction and radiation heat transfers, (ii) allow the modeling of the radiative transfer in anisotropy system such as an assembly of cylinders, and (iii) have an easy numerical implementation into the energy equations of the porous media. In order to study the accuracy of the approach, the paper evaluates the model for porous media composed of spheres or cylinders. The predictions of the model agree well with experimental data and with results obtained from finite element simulations. The numerical results also show that the radiative conductivity can be strongly influence by the effect of temperature distribution across the particle surface and by the effect of the multiple scattering of radiation in the porous media.

Résumé

Un modèle théorique pour évaluer le tenseur de conductivité radiative d'un milieu poreux est développé dans cet article. Le milieu poreux est composé par un fluide transparent et par des particules opaques dont la taille caractéristique est beaucoup plus grande que la longueur d'onde du rayonnement thermique. Les caractéristiques principales du modèle proposé sont : (i) de tenir compte de l'interaction entre les transferts thermiques par conduction et par rayonnement, (ii) de permettre de modéliser le transfert radiatif dans des milieux anisotropes tels qu'un arrangement des crayons, et (iii) d'avoir une implémentation numérique simple dans les équations de bilan d'énergie du milieu poreux. Pour étudier la précision de cette approche, ce travail évalue le modèle dans le cas des milieux poreux composés de sphères ou de cylindres. Les prédictions du modèle sont en bon accord avec les données expérimentales ainsi qu'avec les résultats obtenus à partir des simulations par la méthode des éléments finis. Les résultats numériques montrent de plus, que la conductivité radiative est fortement influencée par l'effet de la distribution de la température à la surface des particules et par l'effet des multiples réflexions du rayonnement dans le milieu poreux.

Keywords: Porous media; Radiation; Equivalent conductivity; Anisotropy; Nuclear reactor

Mots-clés : Milieux poreux ; Rayonnement ; Conductivité équivalente ; Anisotrope ; Réacteur nucléaire

1. Introduction

A severe nuclear reactor accident similar to Three-Mile Island is characterized by a loss of core coolant and relative high core temperatures. During the severe accident the reactor core geometry can degrade in several ways. In the pressurized water reactors (PWRs), the fuel rods will be heated by the residual nuclear power and by the exothermic chemical reactions between the fuel rod cladding and the steam. If the remaining core cooling is insufficient, the fusion temperature of core material can be reached. Then the partial or total fusion of the fuel rod can transform certain regions of the core into thick debris beds of rubble or degraded rod bundles [1].

Current safety analysis attempts to predict the final reactor state scenario. To model the behavior of the PWR core

* Correspondence and reprints.
E-mail addresses: prubiolo@libertysurf.fr, rubiolpr@westinghouse.com (P. Rubiolo), gatt@drncad.cea.fr (J.-M. Gatt).

1290-0729/02/$ – see front matter
PII: S1290-0729(02)01332-7

Nomenclature

a_x, a_y	absorption coefficients for the X and Y directions, respectively	
$\hat{a}$, $\hat{r}$, $\hat{t}$	absorption, reflection and transmission coefficients corrected by the effect of the temperature distribution	
d	characteristic length of the particles	m
E	thermal emission of the layer	$W{\cdot}m^{-2}$
f^+, f^-	view factors	
F	normalized radiative conductivity	
I	intensity of radiation	$W{\cdot}m^{-2}$
$\boldsymbol{Kr}$	radiative conductivity tensor	$W{\cdot}m^{-1}{\cdot}K^{-1}$
Krx	radiative conductivity coefficient in X direction	$W{\cdot}m^{-1}{\cdot}K^{-1}$
Kry	radiative conductivity coefficient in Y direction	$W{\cdot}m^{-1}{\cdot}K^{-1}$
Kt	equivalent conductivity	$W{\cdot}m^{-1}{\cdot}K^{-1}$
$Kcell$	thermal conductivity of the unit cell without radiation	$W{\cdot}m^{-1}{\cdot}K^{-1}$
$Kr_{\perp}$	radiative conductivity in the perpendicular direction to the cylinders	$W{\cdot}m^{-1}{\cdot}K^{-1}$
$Kr_{//}$	radiative conductivity in the parallel direction to the cylinders	$W{\cdot}m^{-1}{\cdot}K^{-1}$
k_s	solid conductivity	$W{\cdot}m^{-1}{\cdot}K^{-1}$
k_f	fluid conductivity	$W{\cdot}m^{-1}{\cdot}K^{-1}$
k_s^*	dimensionless solid conductivity	
N_S	number of cylinders per unity of length	m^{-1}
p	porosity	
p_e	perimeter of bundle	m
qx	component of the radiative flux in X direction	$W{\cdot}m^{-2}$
qy	component of the radiative flux in Y direction	$W{\cdot}m^{-2}$
$\boldsymbol{q^r}$	net radiative flux vector	$W{\cdot}m^{-2}$
r_x, r_y	fractions reflected backwards in relation to the radiative flux	
r_{xy}, r_{yx}	fractions reflected transversally in relation to the radiative flux	
$\boldsymbol{r_s}$	position vector	m
$Sx_{i,j}$	surface of the elementary volume ij in the X direction	m^2
$Sy_{i,j}$	surface of the elementary volume ij in the Y direction	m^2
S	cross bundle area	m^2
T	temperature	K
t_x, t_y	transmissivity coefficients	
$\overline{T}$	average temperature	K
T_∞	particle temperature when k_s^* tends to infinite	K
T_o	particle temperature when k_s^* tends to zero	K
$\hat{x}$, $\hat{y}$, $\hat{z}$	unitary vectors	K

Greek symbols

ε	particle emissivity	
ε_w	wall emissivity	
λ	radiation wavelength	m
σ	Boltzman constant	$W{\cdot}m^{-2}{\cdot}K^{-4}$
π^+, π^-	bounding planes of the unity cell	
Δx	layer thickness in X direction	m
Δy	layer thickness in Y direction	m

Subscripts

i	subscript for the discretization in the X axis
j	subscript for the discretization in the Y axis

Superscripts

$+$	positive sense for a given direction
$-$	negative sense for a given direction
r	net radiative flux

during a severe accident, an estimation of the heat removal capability of the core is required. This capability will vary greatly for the geometry of the intact core region and the damaged regions (debris beds and damaged rod bundles). In addition, due to the high predicted rod temperatures, a considerable amount of energy will be removed by radiative transport. Therefore an accurate thermal model of the core must include the changes of core geometry during the accident and the radiative contribution to total heat transfer.

The evaluation of core thermal behavior can be made using the local volume-averaging methods developed for porous medias. The geometry of the intact and low damaged core regions can be approximated by an arrangement of cylinders while the debris bed regions can be treated as a bed of spheres. In addition, the radiative heat transfer in the core can be estimated by using the modeling concept of radiative conductivity. This concept implies that radiative heat transfer through the porous medium can be modeled using a temperature dependent conductivity. This approach is especially useful for low porosity media composed of opaque particles such as the fuel rod arrangements of the core or the debris beds formed during the severe accident. With the radiative conductivity coefficient, the radiative heat transfer component can be easily included into the volume averaged energy equations. However, an important limitation is the difficulty of evaluating this coefficient.

The radiative conductivity can be obtained from different methods of resolution of the radiative transfer equation [2,3] (two-flux approximation, multiple layer approach, Monte Carlo method, etc.). Among these methods, the multiple layer approach appears to be the most promising since it allows one to readily determine the radiative properties of a medium geometry. However, the multiple layer method was designed for a one-dimensional temperature field while the

analysis of this paper features a two-dimensional temperature field. In addition, the multiple layer method supposes that the temperature in the particles is constant. Therefore it does not take into account the interaction between radiative heat transfer and thermal conduction. Accordingly, a new model which allows the determination of the radiative conductivity of a porous media is developed in this work.

The paper is organized as follows. Section 2 starts writing the radiant energy balance for an elementary volume taking into consideration the fact that there are two independent directions in the porous media. From this radiant energy balance, the radiative conductivity tensor is obtained. Subsequently, a correction on the radiative conductivity is introduced to account for the effect of the temperature distribution across the particle surfaces. Finally, the radiative conductivity is used to calculate the equivalent conductivity of the medium. Therefore the radiative transfer can be included in the energy equations through this equivalent conductivity. In other respects, as the geometry of the intact core can be approximated by an arrangement of cylinders and the debris bed region can be treated as a bed of spheres, in Section 3, we evaluate the proposed model for these type of particles. To do that, the radiative properties of spheres and cylinders are needed. Therefore a correlation for calculating the radiative properties for cylinders is proposed while for the spheres we use the correlation of Mazza [4]. Then using these correlations, the radiative conductivity of arrays of spheres or cylinders are calculated for different values of porosity, emissivity and thermal conductivity of the particles. In Section 3 the model predictions are also compared with results obtained from: (i) the Monte Carlo method by Kaviany [2] for a bed of spheres, (ii) the two flux method, and (iii) numerical calculations using a finite elements method for arrays composed of cylinders. Lastly, a comparison is performed between the predicted and the experimentally-measured equivalent conductivity (i.e., conduction and radiation) for a porous media composed of spheres. Section 4 presents the conclusions.

2. Analysis

2.1. Radiative conductivity tensor

The solution of the equation of the radiative transfer requires the knowledge of radiative properties of the medium, i.e., the absorption and scattering coefficients and the scattering phase function [5,6]. The radiative properties can be calculated using the theory of independent scattering or the theory of dependent scattering. The first theory assumes that the interaction between radiation and particles is not influenced by the presence of neighboring particles. The radiative properties are thus obtained from the properties of individual particles. The second theory considers that the interaction of a given particle with the radiation is affected by the presence of neighboring particles. This mutual dependence between neighboring particles refers to the effect of multiple scattering between particles and mutual interaction with the same incident wave and interference effects. The limits of the theory of independent scattering have been investigated by Kaviany [7]. This author concluded that the theory of independent scattering is not suitable for systems with low porosity and that it can fail to predict the radiative properties of a porous medium even for porosities as high as 0.935. As the porosities of the rod arrangements and the debris beds found in a reactor core are in the range of $0.21 < p < 0.6$ [1], the independent theory is not suitable in our applications and we consider the effect of multiple scattering for calculating the radiative properties of medium.

Another crucial step on the radiation modeling is the choice of the theory used in describing the scattered radiation. The radiation scattered by a particle can be separated into diffracted and reflected components. For large particles ($\pi d/\lambda \gg 1$), the diffracted radiation is concentrated in a small solid angle around the propagation direction, with the angle of peak intensity inversely proportional to particle size. In those cases and for radiative transfer calculations, the diffracted radiation need not to be separated from that which is transmitted and the geometric optics can be applied. Therefore as rods and debris found in the reactor core can be considered as large particles, we calculate the optical properties of the core using the theory of the geometric optics (no interference effects).

The radiative conductivity tensor is now derived, considering that there are two independent directions (the analysis can be extended to three independent directions) and dividing the porous medium in elementary volumes as can be seen on the Fig. 1. In our applications a elementary volume can have different compositions: those placed in the intact or low damaged core regions are composed by fuels rod while those corresponding to the damaged regions are composed by a debris bed. In the analysis the following assumptions are made:

(1) The porous surfaces are opaque and gray. The fluid inside the pores is transparent.
(2) The surfaces and the boundary conditions are diffuse.
(3) The flux on the surface of an elementary volume has hemispherical isotropy characteristics.
(4) The temperature is constant in the elementary volume.
(5) The media is symmetric with respect to the Z axis.

From the schema of the elementary volume of Fig. 1 and integrating the radiative flux over its surfaces, the following fluxes are defined:

$$qx^{\pm}_{i,j} = \frac{1}{Sx_{i,j}} \int_{Sx_{i,j}} \left[\int_{\pm\hat{\boldsymbol{n}}\cdot\hat{\boldsymbol{x}}\geqslant 0} I\left(\boldsymbol{r},\hat{\boldsymbol{n}}\right) \left|\mathrm{d}\hat{\boldsymbol{n}} \bullet \hat{\boldsymbol{x}}\right| \right] \mathrm{d}s$$
$$qy^{\pm}_{i,j} = \frac{1}{Sy_{i,j}} \int_{Sy_{i,j}} \left[\int_{\pm\hat{\boldsymbol{n}}\cdot\hat{\boldsymbol{y}}\geqslant 0} I\left(\boldsymbol{r},\hat{\boldsymbol{n}}\right) \left|\mathrm{d}\hat{\boldsymbol{n}} \bullet \hat{\boldsymbol{y}}\right| \right] \mathrm{d}s \tag{1}$$

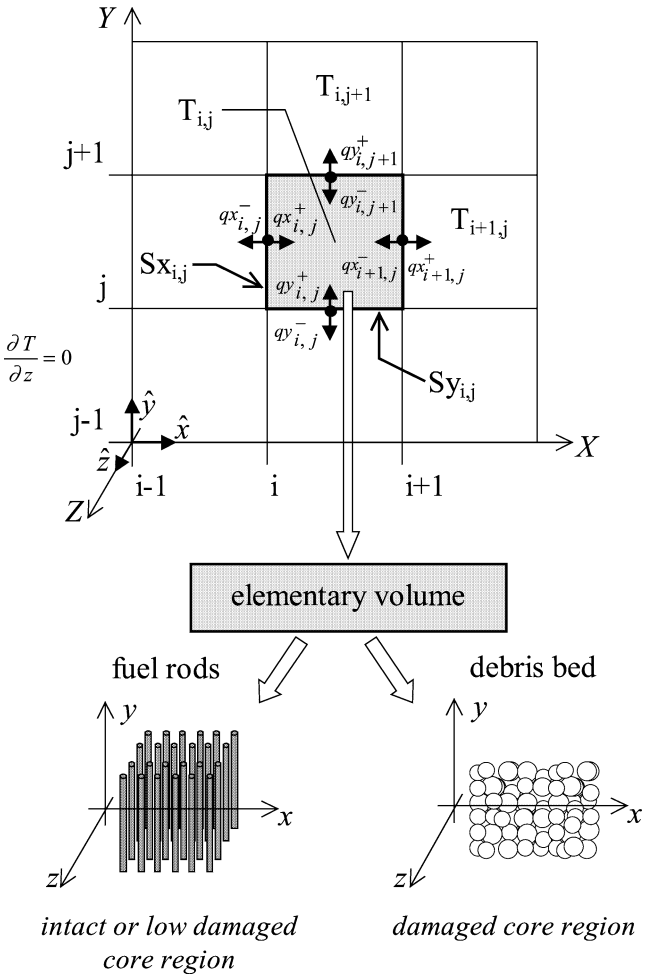

Fig. 1. Schematic illustration of the elementary volume ij and the radiative fluxes. A elementary volume can be composed of a rod assembly (in the intact core region) or a debris bed (in the damaged core region).

where the intensity of radiation I is a function of the position vector $\boldsymbol{r}$ and the direction $\hat{\boldsymbol{n}}$, $Sx_{i,j}$ and $Sy_{i,j}$ are the surfaces of the elementary volume ij and the superindice $\pm$ specifies the sense for a given direction.

Then the radiant energy balance for the volume ij can be written as:

$$\begin{aligned}
qx^{+}_{i+1,j} &= t_x qx^{+}_{i,j} + r_x qx^{-}_{i+1,j} + r_{yx}\Phi x_{i,j} + a_x\sigma T^4_{i,j}\\
qx^{-}_{i,j} &= t_x qx^{-}_{i+1,j} + r_x qx^{+}_{i,j} + r_{yx}\Phi x_{i,j} + a_x\sigma T^4_{i,j}\\
qy^{+}_{i,j+1} &= t_y qy^{+}_{i,j} + r_y qy^{-}_{i,j+1} + r_{xy}\Phi y_{i,j} + a_y\sigma T^4_{i,j}\\
qy^{-}_{i,j} &= t_y qy^{-}_{i,j+1} + r_y qy^{+}_{i,j} + r_{xy}\Phi y_{i,j} + a_y\sigma T^4_{i,j}
\end{aligned} \tag{2}$$

where

$$\begin{cases}
\Phi x_{i,j} = qy^{+}_{i,j} + qy^{-}_{i,j+1}\\
\Phi y_{i,j} = qx^{+}_{i,j} + qx^{-}_{i+1,j}
\end{cases} \tag{3}$$

and σ is the Boltzman constant, t_x and t_y are the transmissivity coefficients for the X and Y directions, respectively, a_x and a_y are the absorption coefficients, r_x and r_y are the flux fractions reflected backwards in relation to the flux direction, and r_{xy} and r_{yx} are the flux fraction reflected in the transversal direction in relation to the flux direction. All these coefficients are defined for the volume ij. The optic coefficients fulfill the following relation:

$$\begin{cases}
1 = t_x + r_x + 2r_{xy} + a_x\\
1 = t_y + r_y + 2r_{yx} + a_y
\end{cases} \tag{4}$$

Eq. (4) expressed the different interactions undergone by the radiative flux in the elementary volume. For example, regarding the radiative flux in the X direction, the first relation of Eq. (4) means that the fraction: (i) t_x is transmitted through the elementary volume, (ii) r_x is reflected backwards in relation to the flux direction, (iii) $2\cdot r_{xy}$ is reflected in the Y direction and (iv) a_x is absorbed in the elementary volume. The same relation is established for the radiative flux in the Y direction by the second relation of Eq. (4).

In obtaining Eqs. (2)–(4), certain symmetries in the radiative properties were assumed. For example, the fraction of energy reflected backwards r_x, is assumed to be the same for $qx^{+}_{i,j}$ and $qx^{-}_{i+1,j}$. In addition, the fraction of energy transversally reflected, r_{xy} (or r_{yx}), is assumed to be equal in both senses of the transversal direction. In the case of an assembly of cylinders, these assumptions are valid if the chosen reference system coincides with the principal directions of the arrangement as can be seen in Fig. 1 (i.e., the parallel and perpendicular direction to the cylinders).

The set of linear equations (2) may be solved simultaneously once the intensities at the boundaries are specified. The terms $\Phi x_{i,j}$ and $\Phi y_{i,j}$ of Eqs. (2) represent a coupling between the radiant energy balances for each direction. In order to obtain the net radiative flux equations, these terms are rewritten using (2) in the following manner:

$$\begin{aligned}
&\left[qx^{+}_{i,j} + qx^{-}_{i+1,j}\right]\\
&\quad = t_x qx^{+}_{i-1,j} + r_x qx^{+}_{i+1,j} + t_x qx^{-}_{i+2,j} + r_x qx^{-}_{i,j}\\
&\qquad + r_{yx}\left[qy^{+}_{i-1,j} + qy^{+}_{i+1,j} + qy^{-}_{i-1,j+1} + qy^{-}_{i+1,j+1}\right]\\
&\qquad + a_x\sigma\left[T^4_{i-1,j} + T^4_{i+1,j}\right]\\
&\left[qy^{+}_{i,j} + qy^{-}_{i,j+1}\right]\\
&\quad = t_y qy^{+}_{i,j-1} + r_y qy^{+}_{i,j+1} + t_y qy^{-}_{i,j+2} + r_y qy^{-}_{i,j}\\
&\qquad + r_{xy}\left[qx^{+}_{i,j-1} + qx^{+}_{i,j+1} + qx^{-}_{i+1,j-1} + qx^{-}_{i+1,j+1}\right]\\
&\qquad + a_y\sigma\left[T^4_{i,j-1} + T^4_{i,j+1}\right]
\end{aligned} \tag{5}$$

Assuming small linear variations of the flux and the temperature profile in the representative volume (for example, $qx^{+}_{i,j-1} + qx^{+}_{i,j+1} \cong 2qx^{+}_{i,j}$ and $T^4_{i,j-1} + T^4_{i,j+1} = 2T^4_{i,j}$), we obtain:

$$\begin{aligned}
\left[qy^{+}_{i,j} + qy^{-}_{i,j+1}\right] &\cong \frac{2r_{xy}}{1-t_y-r_y}\left[qx^{+}_{i,j} + qx^{-}_{i+1,j}\right]\\
&\quad + \frac{2a_y\sigma}{1-t_y-r_y}T^4_{i,j}\\
\left[qx^{+}_{i,j} + qx^{-}_{i+1,j}\right] &\cong \frac{2r_{yx}}{1-t_x-r_x}\left[qy^{+}_{i,j} + qy^{-}_{i,j+1}\right]\\
&\quad + \frac{2a_x\sigma}{1-t_x-r_x}T^4_{i,j}
\end{aligned} \tag{6}$$

Replacing $\Phi x_{i,j}$ and $\Phi y_{i,j}$ by (6), the linear system (2) becomes

$$\begin{aligned} qx^{+}_{i+1,j} &= T_x qx^{+}_{i,j} + R_x qx^{-}_{i+1,j} + A_x \sigma T^4_{i,j} \\ qx^{-}_{i,j} &= T_x qx^{-}_{i+1,j} + R_x qx^{+}_{i,j} + A_x \sigma T^4_{i,j} \\ qy^{+}_{i,j+1} &= T_y qy^{+}_{i,j} + R_y qy^{-}_{i,j+1} + A_y \sigma T^4_{i,j} \\ qy^{-}_{i,j} &= T_y qy^{-}_{i,j+1} + R_y qy^{+}_{i,j} + A_y \sigma T^4_{i,j} \end{aligned} \tag{7}$$

where the new optic coefficients are defined as

$$\begin{aligned} T_x &= t_x + \frac{2r_{yx}r_{xy}}{1-t_y-r_y} & T_y &= t_y + \frac{2r_{xy}r_{yx}}{1-t_x-r_x} \\ R_x &= r_x + \frac{2r_{yx}r_{xy}}{1-t_y-r_y} & R_y &= r_y + \frac{2r_{xy}r_{yx}}{1-t_x-r_x} \\ A_x &= a_x + \frac{2r_{yx}a_y}{1-t_y-r_y} & A_y &= a_y + \frac{2r_{xy}a_x}{1-t_x-r_x} \end{aligned} \tag{8}$$

and they fulfill the relation $A_x + R_x + T_x = 1$ and $A_y + R_y + T_y = 1$. The radiative fluxes in the equations system (7) are not directly coupled as in Eq. (2), but the implicit coupling due to the temperature field remains.

In order to clarify the meaning of Eq. (8) we can consider a one-dimensional temperature field in the X direction (i.e., $\partial T/\partial y = 0$). Then the total transmission t_1 of a layer perpendicular to the X axis is obtained from the following series:

$$\begin{aligned} t_1 &= t_x + 2r_{xy}r_{yx} + 2r_{xy}(t_y + r_y)r_{yx} \\ &\quad + 2r_{xy}(t_y + r_y)^2 r_{yx} + 2r_{xy}(t_y + r_y)^3 r_{yx} + \cdots \\ &= t_x + 2r_{xy}r_{yx}\sum_{n=0}^{\infty}(t_y + r_y)^n \end{aligned} \tag{9}$$

where the limit is $t_1 = t_x + \frac{2r_{xy}r_{yx}}{1-t_y-r_y} = T_x$. In the same manner it can be showed that A_x, R_x, A_y, R_y and T_y represent the uni-dimensional optic coefficients corresponding to a layer perpendicular to the axe considered. Thus for a one-dimensional temperature field, the formulation of the multiple layer method is recovered.

Defining the total radiative flux as

$$\begin{aligned} qx^{r}_{i,j} &= qx^{+}_{i,j} - qx^{-}_{i,j} \\ qy^{r}_{i,j} &= qy^{+}_{i,j} - qy^{-}_{i,j} \end{aligned} \tag{10}$$

and using Eq. (7), the total radiative flux equation is obtained

$$\begin{aligned} qx^{r}_{i+1,j} &= -4\left[\frac{2-(A_x+2R_x)}{A_x+2R_x}\right]\sigma T^3_{i,j}(T_{i+1,j} - T_{i,j}) \\ &\quad + \frac{T_x}{A_x(A_x+2R_x)}\left[\Delta qx^{r}_{i+1,j} - \Delta qx^{r}_{i,j}\right] \\ qy^{r}_{i,j+1} &= -4\left[\frac{2-(A_y+2R_y)}{A_y+2R_y}\right]\sigma T^3_{i,j}(T_{i,j+1} - T_{i,j}) \\ &\quad + \frac{T_y}{A_y(A_y+2R_y)}\left[\Delta qy^{r}_{i,j+1} - \Delta qy^{r}_{i,j}\right] \end{aligned} \tag{11}$$

where $\Delta qx^{r}_{i,j} = qx^{r}_{i+1,j} - qx^{r}_{i,j}$ and $\Delta qy^{r}_{i,j} = qy^{r}_{i,j+1} - qy^{r}_{i,j}$. Provided that: (a) the temperature profile, the sources of power, and the coefficient of convection have smooth responses in the realms of space (the elementary volume) and time, (b) the emissivity of the porous surfaces is not near zero and (c) the medium is optically thick, then the second term on the right-hand side of Eqs. (11) is much smaller than the first one [8,9]. Therefore, outside the reach of the wall radiation, the second term of each equation can be neglected (i.e., we can make a first order approximation for the total radiative flux) and Eq. (11) in rewritten in a tensor form as:

$$\boldsymbol{q^r} = \boldsymbol{Kr}(T) \bullet \nabla T = \begin{bmatrix} -Krx(T) & 0 \\ 0 & -Kry(T) \end{bmatrix} \bullet \nabla T \quad \text{where}$$

$$\begin{cases} Krx = 4\left[\dfrac{2-(A_x+2R_x)}{(A_x+2R_x)}\right]\sigma T^3 \Delta x \\ Kry = 4\left[\dfrac{2-(A_y+2R_y)}{(A_y+2R_y)}\right]\sigma T^3 \Delta y \end{cases} \tag{12}$$

and Δx and Δy are the layer thickness in each direction.

The radiative conductivity tensor obtained in Eq. (12) is diagonal. The coefficients Krx and Kry are the radiative conductivities corresponding to the X and Y directions respectively. These coefficients can be calculated using the optical coefficients of Eq. (7). In addition, as previously showed, Eq. (7) means that the radiative transfer may be analyzed applying independently the multiple layer method in each of the principals directions. Therefore, in order to simplify the notation, we carry out the remainder of the analysis only for one of the principal directions of the medium.

2.2. Effect of temperature distribution across particle surfaces on radiative conductivity

The radiative conductivity obtained in the precedent subsection was derived by assuming in Eqs. (2) and (3), that the temperature distribution across the particle surfaces in the elementary volume is constant. However when the solid conductivity is very small with respect to radiative conductivity, this supposition is no longer valid. The temperature distribution in the particle depends on the particle emissivity ε and the dimensionless solid conductivity k^*_s defined as:

$$k^*_s = \frac{k_s}{4d\sigma\overline{T}^3} \tag{13}$$

where k_s is the solid conductivity, d the characteristic length of the particles (the diameter for spheres or cylinders and the thickness for slabs) and $\overline{T}$ the volume average temperature. The dependence of the temperature distribution with respect to k^*_s and ε is explained because both parameters determine the heat flux through the particle. As previous works [8, 10] show that the radiative conductivity can be strongly influenced by the temperature distribution, in this section a correction is introduced on the optic coefficients to take into account this effect. As explained at the end of Section 2.1 we carry out the analysis for one of the principal directions, that is we consider in our analysis a layer instead of an elementary volume. However the correction proposed in this section can be use for all the optics coefficients of Eq. (7).

For a given volume average temperature $\overline{T}$ we define $T_o(\boldsymbol{r_s})$ as the temperature distribution when k_s^* tends to zero and T_∞ as the temperature distribution when k_s^* tends to infinite (i.e., when the layer is isothermal):

$$\begin{cases} T_o(\boldsymbol{r_s}) = \lim\limits_{k_s^*\to 0} T(\boldsymbol{r_s}) \\ T_\infty = \lim\limits_{k_s^*\to\infty} T(\boldsymbol{r_s}) \end{cases} \tag{14}$$

Then we supposed that, for a given values of k_s^* and ε, the temperature distribution of the particles in the layer can be written as an interpolation between $T_o(\boldsymbol{r_s})$ and T_∞ as follow:

$$T\left(\boldsymbol{r_s}, k_s^*, \varepsilon\right) = \varphi\left(k_s^*, \varepsilon\right) T_o(\boldsymbol{r_s}) + \left(1 - \varphi\left(k_s^*, \varepsilon\right)\right) T_\infty \tag{15}$$

where $\boldsymbol{r_s}$ is the position. The interpolation function φ must satisfy:

$$\begin{cases} \lim\limits_{k_s^*\to 0} \varphi\left(k_s^*, \varepsilon\right) = 1 \\ \lim\limits_{k_s^*\to\infty} \varphi\left(k_s^*, \varepsilon\right) = 0 \\ \lim\limits_{\varepsilon\to 0} \varphi\left(k_s^*, \varepsilon\right) = 0 \end{cases} \tag{16}$$

The first and the second conditions of Eq. (16) are obtained from Eq. (14). The third condition means that there is no heat flux through the particles when the emissivity is zero and then the temperature is constant and equal T_∞. In addition, by definition, the volume average of the temperature distributions T_∞, T_o and T must be equal $\overline{T}$:

$$\overline{T} = \left\langle T\left(\boldsymbol{r_s}, k_s^*, \varepsilon\right)\right\rangle = T_\infty = \left\langle T_o(\boldsymbol{r_s})\right\rangle \tag{17}$$

From consideration of Eqs. (15) and (17), the thermal emissions in the positive and negative sense, E^+ and E^-, respectively, of the layer of Fig. 2 are written as:

$$E^\pm = \int_S f^\pm(\boldsymbol{r_s}) \sigma\varepsilon \left[\overline{T} + \varphi\left(k_s^*, \varepsilon\right)\left(T_o(\boldsymbol{r_s}) - T\right)\right]^4 \mathrm{d}s \tag{18}$$

where $f^+(\boldsymbol{r_s})$ and $f^-(\boldsymbol{r_s})$ are the view factor of each point of the particle surface S from the π^+ and π^- planes, respectively. By using a first order approximation, Eq. (18) can be written as:

$$\begin{aligned} E^\pm = {} & \sigma\varepsilon\left[\int_S f^\pm(\boldsymbol{r_s})\,\mathrm{d}s\right]\overline{T}^4 \\ & + 4\sigma\varepsilon\varphi\left(k_s^*, \varepsilon\right)\overline{T}^3\left[\int_{\partial S}\left[T_o(\boldsymbol{r_s}) - T_\infty\right] f^\pm(\boldsymbol{r_s})\,\mathrm{d}s\right] \end{aligned} \tag{19}$$

From Eq. (19) and defining $C^\pm = \int_S [T_o(\boldsymbol{r_s}) - \overline{T}] f^\pm(\boldsymbol{r_s})\,\mathrm{d}s$, the multiple layer modified equations are derived as:

$$\begin{cases} q_j^- = t q_{j+1}^- + r q_j^+ + E^- \\ \quad = t q_{j+1}^- + r q_j^+ + \sigma a \overline{T}^4 + 4\sigma\varepsilon\varphi\left(k_s^*, \varepsilon\right)\overline{T}^3 C^- \\ q_{j+1}^+ = t q_j^+ + r q_{j+1}^- + E^+ \\ \quad = t q_j^+ + r q_{j+1}^- + \sigma a \overline{T}^4 + 4\sigma\varepsilon\varphi\left(k_s^*, \varepsilon\right)\overline{T}^3 C^+ \end{cases} \tag{20}$$

where t is the transmissivity of the layer, a the absorption and r the fraction reflected backwards in relation to the flux direction.

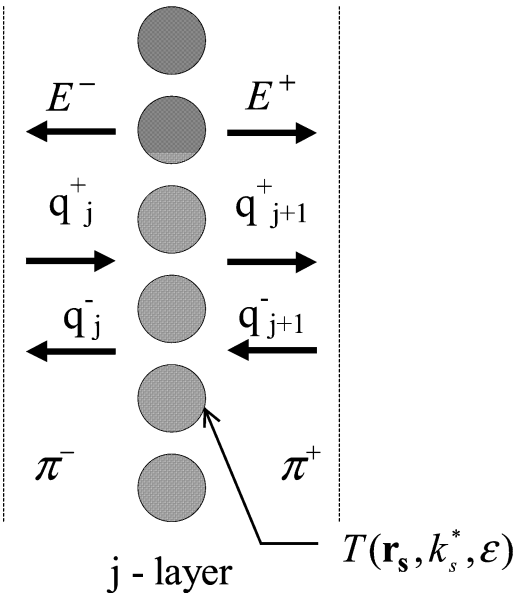

Fig. 2. Schematic illustration of the radiative fluxes and the thermal emissions of an arbitrary layer.

When $k_s^* \to 0$ and $\varepsilon \neq 0$, the particle thermal resistance is bigger than the radiative resistance of the porous media. Then the heat flux through the particles is negligible with respect to the radiative flux outside the particle. Consequently, the radiative energy incident on the particle must be entirely reflected and re-emitted by the surface. In this case the radiation intensity I on the surface of the particles and the optic behavior of the layer are the same as that of a layer with an emissivity equal to zero. Thus the flux can be written as:

$$\begin{cases} q_j^- = t q_{j+1}^- + r q_j^+ + \sigma a \overline{T}^4 + 4\sigma\varepsilon\overline{T}^3 C^- \\ \quad = t_o q_{j+1}^- + r_o q_j^+ \\ q_{j+1}^+ = t q_j^+ + r q_{j+1}^- + \sigma a \overline{T}^4 + 4\sigma\varepsilon\overline{T}^3 C^+ \\ \quad = t_o q_j^+ + r_o q_{j+1}^- \end{cases} \tag{21}$$

where t_o and r_o are the radiative properties for a layer with an emissivity equal a zero. Although the optic behavior of the layer is the same as that of a layer with $\varepsilon = 0$, we note that the layer emissivity is not equal to zero and the temperature distribution in the particles corresponds to T_o.

From Eqs. (21) the value of C^- and C^+ can be obtained. Then the multiple layer modified equations become:

$$\begin{aligned} q_j^- &= \hat{t} q_{j+1}^- + \hat{r} q_j^+ + \sigma \hat{a} \overline{T}^4 \\ q_{j+1}^+ &= \hat{t} q_j^+ + \hat{r} q_{j+1}^- + \sigma \hat{a} \overline{T}^4 \end{aligned} \tag{22}$$

and in the same manner as in obtaining Eqs. (11) and (12) the radiative conductivity can be derived as:

$$Kr\left(k_s^*, \varepsilon\right) = 4\left[\frac{2 - (\hat{a} + 2\hat{r})}{\hat{a} + 2\hat{r}}\right]\sigma \overline{T}^3 \Delta layer \tag{23}$$

where $\Delta layer$ is the layer thickness and the modified radiative properties are defined as:

$$\begin{cases} \hat{a} = a\left[1 - \varphi\left(k_s^*, \varepsilon\right)\right] \\ \hat{r} = r + \varphi\left(k_s^*, \varepsilon\right) \cdot [r_o - r] \\ \hat{t} = t + \varphi\left(k_s^*, \varepsilon\right) \cdot [t_o - t] \end{cases} \tag{24}$$

and they fulfill the relation

$$\hat{a} + \hat{r} + \hat{t} = 1.$$

Given the $\varphi(k_s^*, \varepsilon)$ function, the optic coefficients corrected by the effects of the temperature distribution across the particle surfaces (i.e., solid conductivity effects) are completely determined. This function can be estimated using a simple layer conduction model coupled with the radiation flux over the particle surface. This model supposes that heat flow lines through the layer are parallel to the radiative flux [9]. In the case of layers of spheres, cylinders or a slab we obtain:

$$\varphi(k_s^*, \varepsilon) = \frac{1}{1 + 2\frac{k_s^*}{\varepsilon}}. \tag{25}$$

2.3. Equivalent conductivity

The equivalent conductivity may be obtained from a resistance network approach to the unit cell, using the radiative conductivity *Kr* and the thermal conductivity *Kcell* of the cell. This network is obtained considering the following modes of transfer:

(1) Radiation only: radiative transmission through the free pore section (see Fig. 3).
(2) Alternating thermal conduction and radiation transfer: conductive transfer through the solid phase, coupled with the radiation and conduction in the gas phase.
(3) Pure thermal conduction: thermal transfer by conduction through the gas in the free pore section.

In obtaining the resistance network, we consider that radiative resistance can be decomposed into two different contributions: the resistance associated with radiative flow crossing the layer by direct transmission or multiple reflections R_{radp} and that associated with radiative energy absorbed and re-emitted by the solid particles in the layer R_{rads}. In our resistance model heat transfer is possible between solid particles of adjacent layers by a contact resistance R_c or through gas conduction R_{gas}. The resistance associated with conduction through the particles is denoted R_s while that associated with conduction through the gas in the free pore section is denoted R_p.

From the resistive network of Fig. 3, the total resistance of the layer can be estimated. Considering the extreme cases where $k_s \to 0$ or $T \to 0$ the values of the different resistances can be evaluated and the equivalent conductivity *Kt*, can be expressed as [9]:

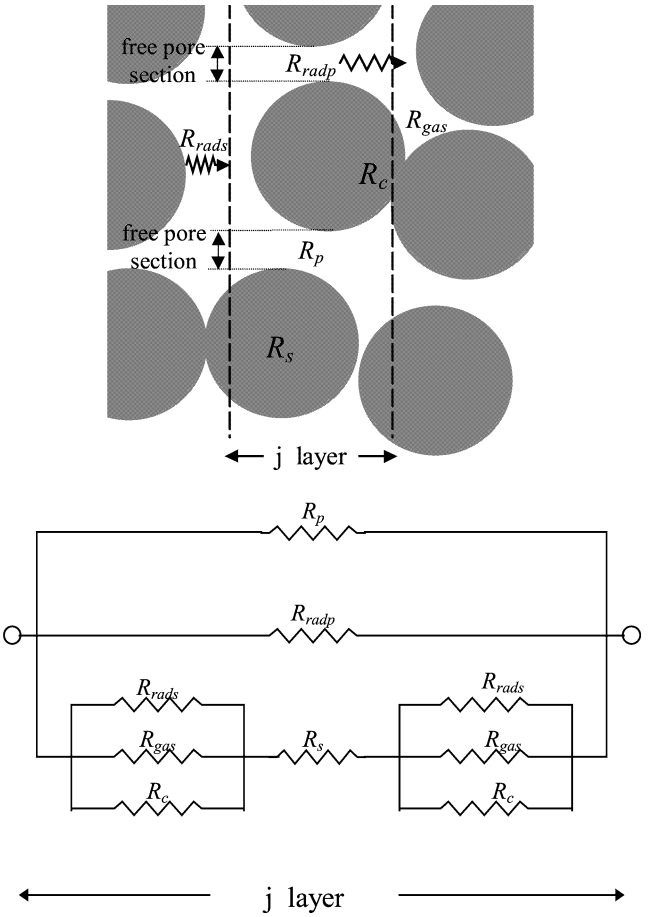

Fig. 3. Resistance network model of the layer.

$$Kt = Kp + Kro + \frac{1}{Rs^* + \frac{1}{\frac{Kr(k_s^*,\varepsilon) - Kro}{1 - Rs^*(Kr(k_s^*,\varepsilon) - Kro)} + \frac{Kcell - Kp}{1 - Rs^*(Kcell - Kp)}}} \tag{26}$$

where $Rs^* = \frac{\varepsilon d r_o^2}{\Delta layer \cdot k_s \cdot [2(r_o - r) - a]}$, $Kro = \mathrm{Lim}_{\varepsilon \to 0} Kr(k_s^*, \varepsilon)$, *Kcell* the thermal conductivity of the cell (i.e., without radiation) and $Kp = 1/R_p$.

If radiation and conduction transfer can be considered as acting in parallel, the Eq. (26) can be simplified as:

$$Kt = Kr(k_s^*, \varepsilon) + Kcell \tag{27}$$

3. Results and discussion

3.1. Evaluation of radiative properties for layers of cylinders

As it was showed by Eq. (7), the radial and axial direction of the arrangement may be analyzed independently. Therefore the radiative properties can be obtained from the resolution of the one-dimensional problem. For the perpendicular direction to the cylinders, the radiative properties can be calculated from the radiative heat exchange between a layer of

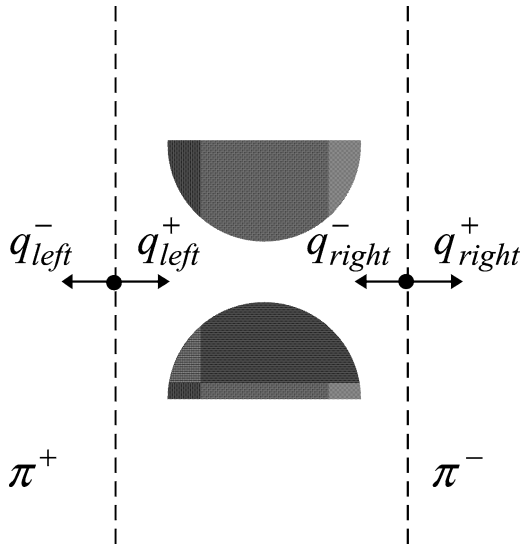

Fig. 4. Unity cell used in the radiative properties calculations.

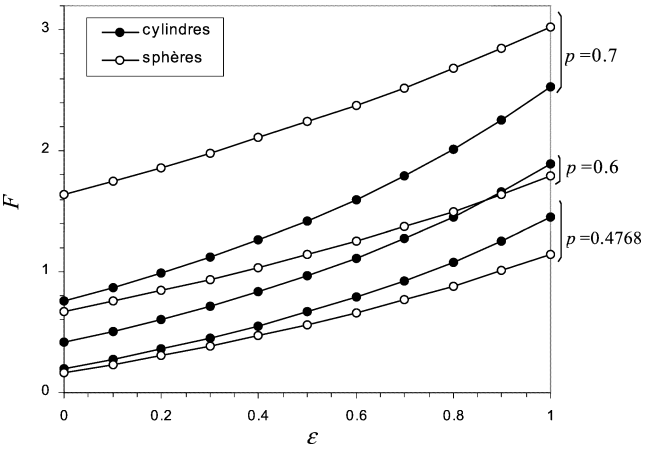

Fig. 5. Variation of the normalized radiative conductivity $F = Kr/4\sigma dT^3$ with respect to emissivity and porosity for beds composed of cylinders or spheres.

infinitely long cylinders and two bounding planes (π^+ and π^-). The array type (i.e., squared or triangular arrays) has not influence on the cylinder disposition in the layer but it changes the effective thickness of the layer. Since each rod in the layer sees only the two neighboring rods, the radiative behavior was calculated from an elementary unit cell like that of Fig. 4. Fixing the particles temperature equal to zero, the layer transmissivity t_l and reflectivity r_l can be obtained from:

$$t_l = \frac{q^+_{\text{right}}}{q^+_{\text{left}}} \quad \text{and} \quad r_l = \frac{q^-_{\text{left}}}{q^+_{\text{left}}} \tag{28}$$

where q^+_{left} and q^-_{left} are the input and output radiative flux on the π^+ plane and q^+_{right} is the output radiative flux on the π^- plane.

The calculations were performed by using the finite element code Castem 2000. Angular flux discretization and meshing were fixed at a value where the variations of the radiative properties arising from the discretization were below 1%. A data base of the radiative properties was built changing the emissivity (twelve values between 0.05 and 1) for different porosities (nine values between 0.22 and 0.95). This data base was fitted with the following correlation:

$$\begin{cases} t = 1 - a - r \\ r = \dfrac{3\pi(1-\varepsilon)N_s(p)\,d\beta}{8} \\ a = \dfrac{\pi\varepsilon N_s(p)\,d\alpha}{2} \end{cases} \tag{29}$$

where p is the porosity, d is the diameter, $N_s(p)$ is the number of cylinders per unity of length ($N_s(p) = \frac{1}{d}\sqrt{\frac{4}{\pi}(1-p)}$ for a cubic array), and α and β are corrections on the radiative properties to account the effect of multiple scattering. These corrections are defined as:

$$\begin{cases} \alpha = \left(1 + \dfrac{1.501\varepsilon + 0.140}{1 + 0.118\varepsilon} \cdot \left(N_s(p)\cdot d\right)^{2.033}\right)^{-0.5} \\ \beta = \left(1 + \dfrac{0.918\varepsilon + 0.388}{1 + 0.156\varepsilon} \cdot \left(N_s(p)\cdot d\right)^{2.095}\right)^{-0.5} \end{cases} \tag{30}$$

Eq. (30) is written using the same general form of the correlation of Mazza et al. for layers of spheres [4].

Using Eqs. (29) and (30) the absorption, reflection and transmission coefficients for the perpendicular direction to a layer of cylinders can be calculated. The proposed correlations are function of the porosity p, the emissivity ε and the cylinder diameter d. The mean squared relative error deviation between the correlations and the data is 1.5% for the reflection coefficient and 2% for absorption coefficient for $0.22 \leqslant p \leqslant 0.95$ and $0.05 \leqslant \varepsilon \leqslant 1$. In addition, the correlations tend to the scattering pattern of an isolated cylinder when it is extrapolated to porosities near zero (i.e., $N_s(p) \to 0$). Finally, Eq. (30) shows that the effect of the multiple scattering can be important even for high porosities. This conclusion is in agreement with that of Kaviany [7].

It is an interesting exercise to use Eqs. (29) and (30) for calculating the radiative conductivity in the perpendicular direction to an assembly of cylinders $Kr_\perp$, and then compare it with that of a bed of spheres. Fig. 5 shows the value of the normalized radiative conductivity $F = \frac{K_r}{4\sigma dT^3}$ obtained for these two porous media using different values of emissivity and porosity. In all cases, the value of Kr was calculated considering the particles as isothermal (i.e., using Eq. (12)). For evaluating Kr for the bed of spheres, we used the radiative properties obtained by Mazza et al. [4] for spherical particles. Fig. 5 shows that for low porosities the values of Kr are strongly dependent upon the particle's emissivity, but weakly dependent upon the particle's shape.

In regards to the parallel direction to the rod bundle, we can obtain an estimation of $Kr_{//}$ considering that $\frac{\partial q_y^{\pm}}{\partial x} \cong 0$ in

the elementary volume. Then using the multiple layer theory, we obtain:

$$Kr_{//} = \frac{16\sigma S(y)}{p_e(y)} T^3 \tag{31}$$

where $S(y)$ is the cross bundle area, $p_e(y)$ is the perimeter and y is the position. In this case no solid conductivity correction on $Kr_{//}$ is needed, because outside the wall radiation, radiative transfer and axial conduction can be considered as acting in parallel. Eq. (31) allows us to make an estimation of the order of magnitude of $Kr_{//}$. When this equation is evaluated with the characteristic values of $S(z)$ and $P(z)$ for reactor rod arrangements, the resulting radiative conductivity $Kr_{//}$ is smaller than the axial thermal conductivity. Therefore the radiative contribution on the equivalent conductivity for the parallel direction to the rod bundle may be neglected in reactor core applications.

3.2. Effect of the temperature distribution across particle surfaces on radiative conductivity

The stationary problem with adiabatic conditions in the upper and lower boundaries of the unit cell of Fig. 4 was solved using a finite element method. The energy transport through this cell is due to radiative transport outside the particles and thermal conduction inside the particles. The finite elements calculations were performed considering no thermal conduction between the cylinders in order to analyze the dependence of the radiative conductivity with respect to the temperature distribution over the particle surfaces.

The mesh discretization was fixed at a value where the variations of the radiative conductivity arising from the discretization were below 1%. Fig. 6 shows the numerical results obtained for the normalized radiative conductivity in the perpendicular direction to the assembly of cylinders using different values of porosity and emissivity. It is also showed in Fig. 6, the predicted values calculated from Eqs. (23)–(25), (29) and (30). The model well predicts the numerical results with a computational cost much smaller than that of the finite element method.

The Fig. 6 shows that the normalized radiative conductivity increase with the value of k_s^* and the emissivity. This can be explained because in the limit when $k_s^* \to \infty$ the temperature inside the particles is almost constant. Therefore, it can be considered that the radiative flux absorbed by an arbitrary element of surface is uniformly emitted by all of the particle's surface. Then the radiative conductivity is augmented. When $k_s^* \to 0$ almost non conduction transfer exist through the solid. Therefore, independent of solid emissivity, the radiation flux over an arbitrary point of the surface must be entirely removed by reflection and thermal emission. Since, radiation cannot cross the solid, the resulting radiative conductivity is lower than before.

Fig. 7 shows the results obtained by Kaviany et al. for layer of spheres [10] using the Monte Carlo method. These results are compared with those obtained by Eqs. (23)–(25)

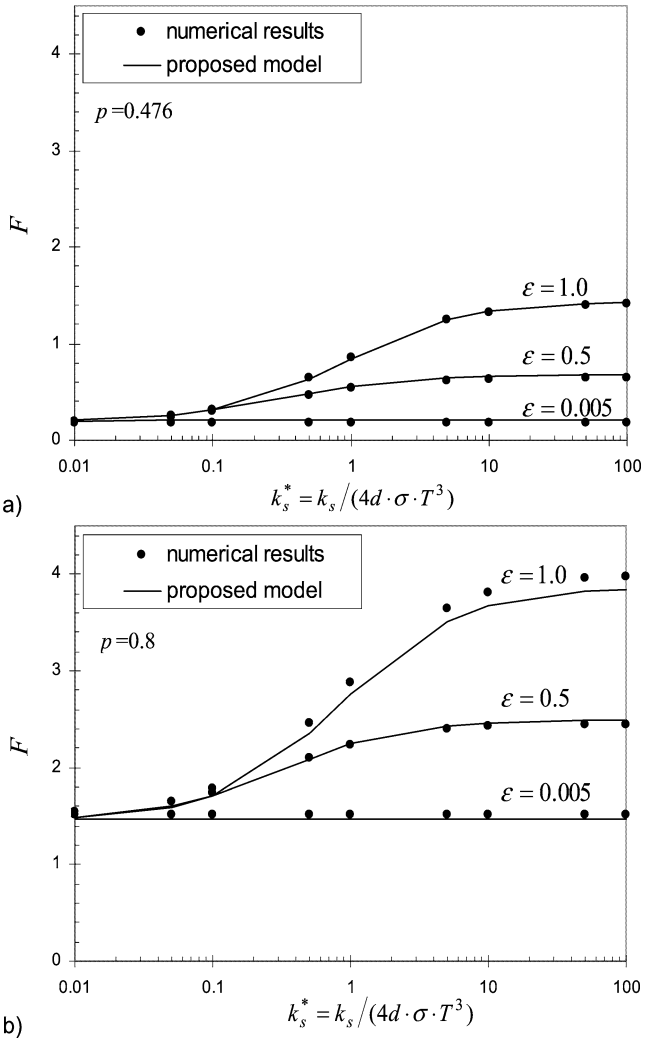

Fig. 6. Variation of the normalized radiative conductivity $F = Kr_{\perp}/4\sigma dT^3$ with respect to the normalized solid conductivity for assemblies of cylinders: (a) $p = 0.476$ and (b) $p = 0.8$.

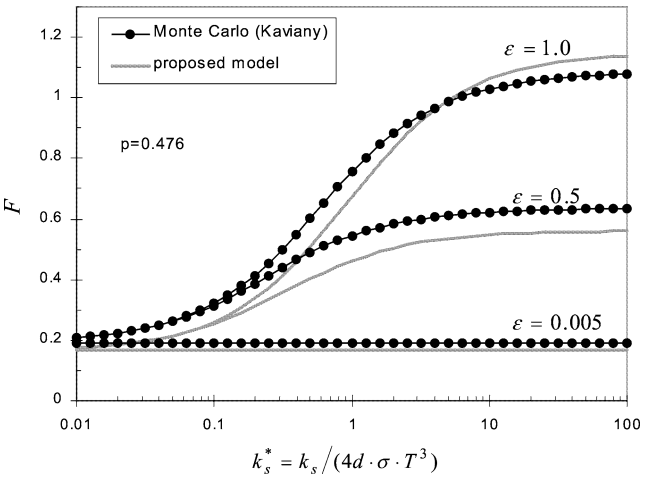

Fig. 7. Variation of the normalized radiative conductivity $F = Kr/4\sigma dT^3$ with respect to the normalized solid conductivity for a bed composed of spheres with $p = 0.476$. Comparison between the proposed model and the results obtained from a Monte Carlo simulation by Kaviany.

using the radiative properties calculated by Mazza et al. [4]. The predictions of the model agree well with the Monte Carlo simulations.

3.3. Comparison of model predictions with experimental results for a packed bed of spheres

The radiative conductivity calculated from Eq. (12) for an uni-dimensional temperature field is compared with the results obtained from the experiment of Kasparek [8]. This experiment measured the normalized radiative conductivity F for a packed bed. The packed bed consisted of polished steel spheres ($\varepsilon = 0.35$) or chromium oxide-coated spheres ($\varepsilon = 0.85$). The spheres were soldered in layers forming an approximately cubic arrangement. The porosity of the bed was 0.4 and the spheres' diameter was 1 cm. Conduction and convection were eliminated by placing the layers a small distance apart and by performing the experiment in vacuum. As the result of the high thermal conductivity of steel, the spheres in each layer can be considered isothermal ($k_s^* \to 0$). A heat source was supplied in the center of the bed. Table 1 shows the normalized radiative conductivity obtained from the Kasparek results and from Eq. (12) evaluated with Mazza coefficients. It is also showed the normalized radiative conductivity obtained from the Monte Carlo Method (diffused scattering) by Kaviany [11], the two flux model and different cell models described by Vortmeyer [8]. Predictions of Eq. (12) are favorably compared with the experimental results.

In Table 1, the normalized radiative conductivity obtained from the two flux method was calculated using the optic coefficients derived by Brewster and Tien for opaque, diffusely reflecting spheres. These coefficients were obtained considering no interaction between particles, i.e., using the independent scattering theory. Therefore, the failure of the independent theory for the lower porosities explains the differences found in the Table 1 between the radiative conductivity obtained from the two flux model with respect to the others models. In other respects, since the independent theory gives good predictions for highly porous systems, Fig. 8 compares the normalized radiative conductivity obtained from Eq. (12) (which takes into account multiple-scattering effects) and from the two flux method for beds of spheres with $p \geqslant 0.8$. As was expected, when the porosity $p \to 1$, the agreement between the results from both methods is better than for lower porosities.

Local measurement of equivalent conductivities *Kt* (i.e., taking into account the conduction and radiation transfers) in packed beds with stagnant air were made by Beveridge and Haughey [12]. The bed consisted of alumina silicate balls. The bed porosity was 0.399 and the balls' diameter was 6 mm. Using their thermal conduction model (i.e., the value of *Kcell*), Eq. (26) was evaluated for a rhonbohedral array of spheres. The equivalent conductivity *Kt*, normalized with the fluid conductivity k_f, is presented in Fig. 9. Due to the uncertainties of the surface emissivity (which is temperature dependent), the results are plotted in Fig. 9 for two values of emissivity. In all of the models, the agreement between calculations and experiment results is quite satisfactory.

Table 1
Normalized radiative conductivity F for a packed bed

Model	Emissivity				
	0.2	0.35	0.60	0.85	1.0
Kasparek	–	0.54	–	1.02	–
Eq. (12)	0.31	0.43	0.66	0.94	1.15
Two-flux	0.88	0.91	0.98	1.06	1.11
Monte Carlo	0.32	0.45	0.68	0.94	1.10
Laubitz	0.27	0.46	0.79	1.13	1.32
Vortmeyer	0.25	0.33	0.54	0.85	1.12
Wakao and Kato	0.21	0.37	0.65	0.96	1.15
Schotte	0.2	0.35	0.6	0.85	1.0

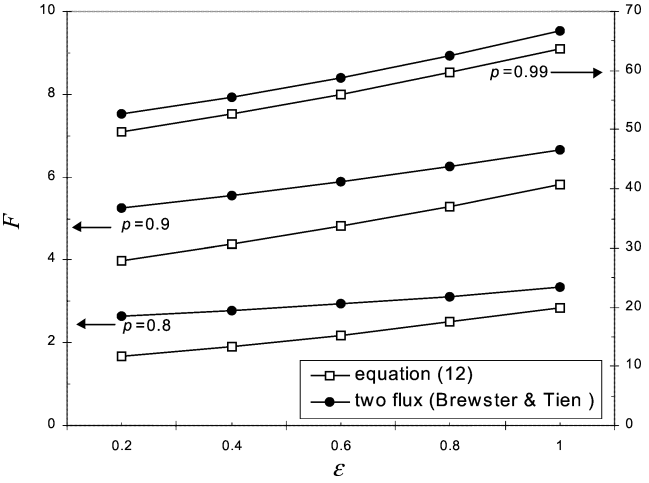

Fig. 8. Normalized radiative conductivity $F = Kr/4\sigma dT^3$ for a bed composed of spheres. Comparison between two-flux and results from Eq. (12) for high porosities.

4. Conclusions

A theoretical model for predicting the radiation contribution to total heat flow in a porous media composed of a transparent fluid and opaque particles was developed. The radiative heat transfer through this medium was calculated by means of a radiative conductivity tensor. This radiative conductivity tensor was evaluated from the absorption, reflection and transmission coefficients of a layer of the medium. Then using a resistance network analogy of a unit cell, the equivalent conductivity tensor of the medium was obtained. The accuracy of the proposed model was evaluated for porous media composed of spheres or cylinders. The predictions of the model agree well with experimental data and with results obtained from finite element simulations. Some conclusions that can drawn from this study are:

(1) The proposed model is well adapted for estimating radiative transfer for the different reactor core configura-

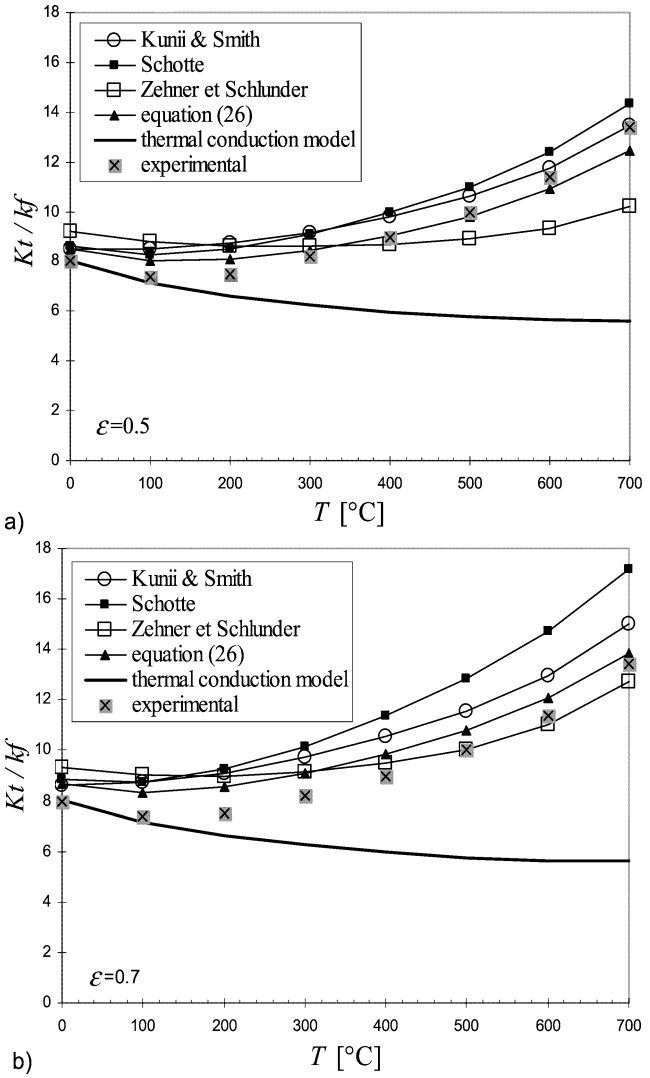

Fig. 9. Experimental curve of Beveridge and Haughey for the normalized equivalent conductivity Kt/k_f compared with results of Eq. (26) and others models: (a) $\varepsilon = 0.5$ and (b) $\varepsilon = 0.7$.

tions found in a severe accident (i.e., for a porous media composed of spheres or cylinders) and for a wide range of porosities and emissivities.

(2) The model seems to allow the determination of the radiative conductivity with an accuracy similar to a finite element method but with a significant reduction in computational cost. Furthermore, the proposed model can be easily included into the energy equations.

(3) The optical coefficients were determined in this work using the theory of dependent scattering. The numerical results show that for the characteristic porosities of the rod arrangements ($0.21 < p < 0.6$), the multiple scattering between the particles must be taken into account. The results also show that the theory of independent scattering can be apply only when the porosity $p \to 1$.

(4) The finite element calculations reveal that the radiative conductivity is strongly dependent of the dimensionless solid conductivity $k_s^* = k_s/(4d\sigma\overline{T}^3)$. Due to the significant variations of the temperatures and the conductivities of materials found in the core during the severe accident, this effect must be taken into account. The proposed model seems to well estimate it.

(5) For low porosities arrangements, the radiative conductivity is more dependent upon the particle's emissivity instead of its shape (spherical or cylindrical).

Subsequent studies during fast transient are needed to validate the radiative conduction approach.

Acknowledgements

P. Rubiolo acknowledges with gratitude the Ph.D. scholarship provided by the Instituto Balseiro-Universidad Nacional de Cuyo, Argentine. This work was performed at the Direction d'Etudes des Réacteurs of CEA. The authors are also grateful for the useful discussions with Professor Roger Martin.

References

[1] J.M. Broughton, P. Kuan, D.A. Petti, E.L. Tolman, A scenario of the three mile island unit 2 accident, Nuclear Technol. 87 (1989) 34–53.
[2] M. Kaviany, Principles of Heat Transfer in Porous Media, Springer-Verlag, New York, 1994.
[3] G.D. Mazza, S.P. Bressa, G.F. Barreto, On the validity of the addition of independent contributions for evaluating heat transfer rates in gas fluidized beds, Powder Technol. 90 (1997) 1–11.
[4] G.D. Mazza, C.A. Berto, G.F. Barreto, Evaluation of radiative heat transfer properties in dense particulate media, Powder Technol. 67 (1991) 137–144.
[5] H.C. Hottel, A.F. Sarofim, Radiative Transfer, McGraw-Hill, New York, 1967.
[6] M.Q. Brewster, Thermal Radiative Transfer and Properties, Wiley-Interscience, New York, 1992.
[7] B.P. Singh, M. Kaviany, Independent theory versus direct simulation of radiation heat transfer in packed beds, Internat. J. Heat Mass Transfer 34 (1991) 2869–2882.
[8] D. Vortmeyer, Radiation in packed solids, in: Proceedings of the 6th Internat. Heat Transfer Conf., Vol. 6, 1978, pp. 525–539.
[9] P. Rubiolo, Modélisation du transfert thermique dans un milieu poreux: application aux réacteurs nucléaires en situation accidentelle, Thèse, Université de Aix-Marseille I, 2000.
[10] B.P. Singh, M. Kaviany, Effect of solid conductivity on radiative heat transfer in packed beds, Internat. J. Heat Mass Transfer 37 (1994) 2579–2583.
[11] B.P. Singh, M. Kaviany, Modelling radiative heat transfer in packed beds, Internat. J. Heat Mass Transfer 35 (1992) 1397–1405.
[12] G.S.G. Beveridge, D.P. Haughey, Axial heat transfer in packed beds, Internat. J. Heat Mass Transfer 14 (1971) 1093–1113.